

BASALT CARBONATISATION AND ITS IMPLICATIONS FOR ANTIMONY MINERALISATION IN NORTH CORNWALL

R. CLAYTON

Clayton, R. 1993. Basalt carbonatisation and its implications for antimony mineralisation in north Cornwall.

Proceedings of the Ussher Society, **8**, 105-111.



A recently discovered style of Sb sulphosalt mineralisation in north Cornwall occurs within a metasomatic rock generated by shear-related carbonatisation of basaltic volcanics. Zones of metasomatic fragmentite acted as loci for progressive outward carbonatisation and Pb-Sb/Cu-Sb sulphosalt mineralisation. The alteration (silicification, chloritisation and carbonatisation) shows similarity to processes of listvenitisation and involved the infiltration of a CO₂-rich fluid. Geochemical changes reflect high CO₂ activity whilst molar CO₂/CaO values indicate dol/dol+cal between 0.13 and 1.02. Paragenetic mapping of the carbonate-chlorite-sulphide assemblage suggests fluctuating conditions, but characterised by a general rise in fluid pH and fO₂ during the final stages of metasomatism. These changes, driven by H⁺ extraction and CO₂ outgassing, effectively generated mild fluid alkalinity and conditions favourable for the mobilisation of Sb, Zr, Y and Ti. The metasomatic/mineralising fluid (CO₂(CH₄)-H₂O-NaCl) evolved via progressive loss of CO₂ during the Pb-Sb-carbonate event (T < = 270°C and P < 750b) to produce a dominantly aqueous fluid.

R. Clayton, Earth Resources Centre, Exeter University, EX4 4QE.

INTRODUCTION

The effect of CO₂ metasomatism in north Cornwall is well developed in basaltic volcanics, where carbonatisation accompanied the transition from ductile to brittle deformation during late Variscan uplift of the northern zone of the Trevone Basin. The distribution of extensive carbonatisation in brittle deformed metabasite is structurally controlled, decreasing in intensity with distance from breccia and shear zone margins. An associated sulphosalt and base metal sulphide mineralisation occurs in an area of carbonatised and brecciated metabasite, ca. 50 x 50m, exposed in low cliff sections at Port Quin [SW 9685 8078]. Here the sulphosalt minerals contribute to the fabric of the metasomatite, in contrast to the more familiar and well developed vein-sulphosalt mineralisation in the surrounding metapelites and metabasites (Clayton et al., 1990).

Field mapping has indicated that carbonatisation is associated with intrabasite, decimetric-scale shear zones (e.g. Port Quin, Stepper Point), or appears to exploit the rheological contrast between metabasites and their surrounding metapelites (e.g. Port

Quin) (Figure 1). Evidence suggests that the structural development of the north Cornish slate-volcanic successions has played an important role in controlling the distribution of carbonatisation. The association of sulphosalt mineralisation accompanying the re-texturing of former ductile structures might imply a genetic link with sulphosalt-carbonate vein mineralisation in this region.

This paper aims to clarify the relationship between the sulphosalt-carbonate assemblage in the metasomatic rock at Port Quin and north Cornish sulphosalt vein mineralisation, and to chart the effects of progressive deformation and carbonatisation upon the geochemistry of the mineralised metabasite at Port Quin. Whole rock geochemistry, with particular reference to high field strength elements, is used to assess the interpretation of some aspects of the geochemical environment at the time of Sb mineralisation.

METABASITE MINERALOGY AND SULPHOSALT MINERALISATION

The primary phase mineralogy is typically clinopyroxene (augite)-plagioclase-ilmenite-apatite (Rice-Burchall, 1991). Multistage alteration, firstly by seafloor processes, then very low grade metamorphism, followed by a metasomatic process, completely restructured the mineralogical framework of the metabasite. The metamorphic assemblage comprises albite-actinolite - quartz - chlorite - sphene - Fe-Ti oxides - (carbonate) - (Fe-sulphide). Primary, accessory apatite appears to have persisted unaltered through the metamorphic event.

The metasomatic rock is composed predominantly of carbonate, chlorite, apatite, white mica, quartz, sulphide/sulphosalt +/- oxide minerals. Relict primary and metamorphic mineral phases were largely overprinted by pervasive carbonatisation. The persistence of relict apatite is conspicuous in parts of the metasomatite, occurring also in veinlets, suggesting some apatite growth during the metasomatic stage.

The different stages of metasomatism, i.e. silicification, chloritisation and carbonatisation, can be satisfactorily correlated with structural observations and petrographic evidence. Brittle-ductile textures in silicified domains and a clear carbonate overprint indicate that silicification preceded carbonatisation. Mineral textures also reveal evidence for alternate pulses of chlorite and carbonate precipitation which characterised the advanced stages of metasomatism. A similarity is noted between this style of alteration

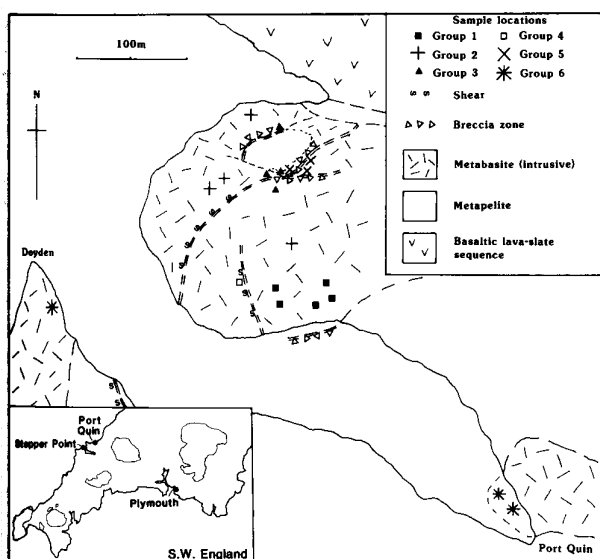


Figure 1: Location map and plan of sample sites.

TABLE 1: Microprobe analyses

		Bi	Pb	Sb	Cd	Ag	As	Zn	Cu	Fe	S	Total
Tet1	wt%	0.19	< 0	30.97	0.04	0.75	< 0	5.56	36.16	1.54	23.83	99.04
	at%	0.15	< 0	15.08	0.02	0.41	< 0	5.04	33.71	1.64	44.04	99.99
Tet2	wt%	0.08	< 0	29.68	1.32	5.07	0.06	< 0	34.59	5.24	22.65	98.69
	at%	0.02	< 0	14.8	0.71	2.85	0.05	< 0	33.02	5.69	42.86	100
Bnt1	wt%	n.d.	43.52	26.23	0.16	n.d.	0.43	n.d.	9.86	0.09	19.25	99.54
	at%	n.d.	17.44	17.9	0.12	n.d.	0.47	n.d.	12.88	1.34	49.84	99.99
Bnt2	wt%	n.d.	45.51	26.22	0.06	0.03	0.54	< 0	9.08	0.15	18.86	100.5
	at%	n.d.	18.31	17.93	0.04	0.02	0.6	< 0	11.89	2.24	48.96	99.99
Bnt3	wt%	n.d.	44.1	26.32	0.1	0.03	0.53	< 0	9.49	0.02	19.11	99.68
	at%	n.d.	17.99	18.28	0.08	0.03	0.6	< 0	12.62	0.03	50.38	100.01
Bnt4	wt%	n.d.	43.67	26.06	0.08	< 0	0.53	< 0	9.91	0.12	18.97	99.34
	at%	n.d.	17.83	18.11	0.06	< 0	0.6	< 0	13.19	0.18	50.04	100.01

n.d. not determined

Cambridge Instruments Microscan 9 electron microprobe (wavelength dispersive spectrometer). Accelerating voltage = 20 kv, spot size 1 μ , counting times between 10 and 60 seconds, ZAF processed.

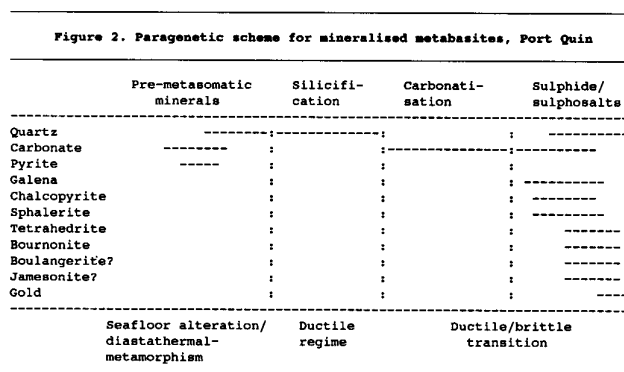


Figure 2: Paragenetic scheme for mineralised metabasites, Port Quin.

this style of alteration and that described by Aydal (1990), and Buisson and LeBlanc (1986) resulting from processes attributed to listvenitisation (sensu Ploshko, 1963).

The metasomatic fragmentite corresponds to thin crosscutting micro-breccias of hydraulic origin and to chemical breccias of varying modal abundances of carbonate, chlorite and quartz. Pb-Sb-Cu-Zn-Fe-Ag sulphide and sulphosal mineralisation accompanied the progressive replacement of the metabasite outwards from these zones. Table 1 shows representative analyses of the common sulphosalts which formed syn- and post-carbonatisation (Figure 2), occurring also in veins at the sheared margins of pelitic enclaves within the metabasite.

The sulphide/sulphosal mineralisation comprises galena, chalcopyrite, sphalerite, tetrahedrite, bournonite, thin acicular sulphosalts (probably jamesonite or boulangerite) and subordinate, resorbed pyrite. Several textural associations within this assemblage show a close resemblance to those described for vein mineralisation (Clayton, 1992):

- The occurrence of bournonite, tetrahedrite and Ag-Sb sulphosal mineral inclusions in galena.
- In galena-free zones, tetrahedrite and bournonite occur in close association, accompanied by other Pb-Sb sulphosalts and small grains of gold.
- Early development of pyrite shows marked textural disequilibrium with other sulphide and sulphosal minerals. A proportion of pyrite may be relict from metamorphic, or earlier alteration, thereby separate from mineralisation that accompanied carbonatisation.
- Carbonatisation appears to be an important precursor stage to sulphosal mineralisation in both veins and the metasomatic rock.

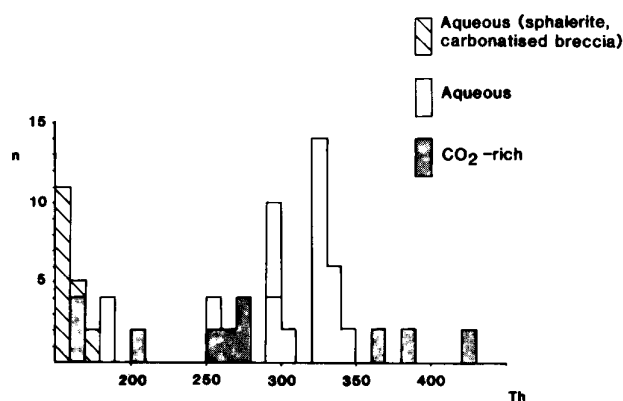


Figure 3: Fluid inclusion homogenisation temperatures.

Two textural generations of carbonate are present; (C1), fine-grained brown carbonate with abundant host rock impurities, and (C2), coarser grained colourless carbonate, clean of impurities. The distribution of sulphide/sulphosal minerals appears to be linked to the replacement of the metabasite by the later stage (C2).

Although a close textural association between sulphosal and carbonate minerals is seen, there is no direct association of this kind between sulphosalts and silicification. In view of the strong carbonate-sulphosal association in discordant vein deposits throughout north Cornwall, this might point to a common CO₂-rich fluid responsible for both metabasite and vein carbonatisation. Inherent in this argument is that both styles of mineralisation were broadly coeval and may have been site-selective in developing only where brittle re-texturing of the rock or vein occurred.

THE METASOMATIC FLUID

Summary data (Figure 3) from fluid inclusion studies in the Port Quin area indicate sulphosal-carbonate mineralisation at T < 270°C and P < 750b from a CO₂-(CH₄)-H₂O-NaCl fluid which evolved via CO₂ loss under falling pressure towards more aqueous compositions (Clayton, 1992). Preliminary studies on inclusions in sphalerite from the metasomatic rock indicate minimum trapping temperatures of 175°C from a low salinity (78 wt % NaCl equivs), CO₂-poor, aqueous fluid (Figure 3).

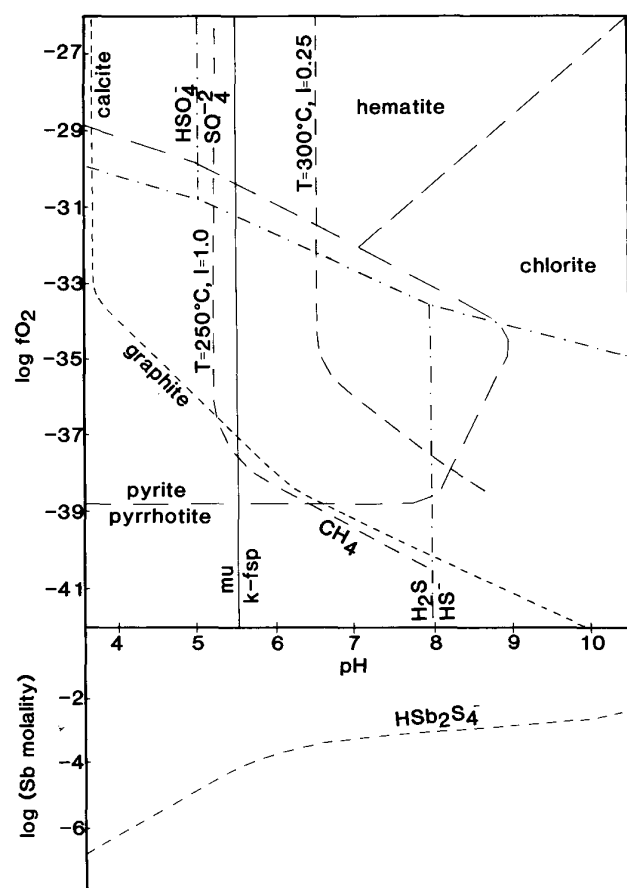
Paragenetically early vein infillings of pyrite-white-mica-K feldspar-quartz indicate pH values close to the Mu - K fsp boundary within the pyrite stability field (Figure 4). Under brittle deformation CO₂ is permitted to escape from the fluid, lowering carbonate solubility and promoting carbonatisation, whilst chlorite mineralisation was effective in extracting H⁺ from the fluid.

TABLE 2: Averaged geochemical (XRF) analyses.

	GROUP 1	GROUP 2	GROUP 3	GROUP 4	GROUP 5	GROUP 6
SiO ₂	49.6	53.31	46.51	53.02	43.02	47.31
Al ₂ O ₃	16.49	16.39	18.99	17.03	8.98	13.52
TiO ₂	2.03	1.84	1.17	2.14	0.61	1.02
Fe ₂ O ₃	11.93	11.53	9.93	12.64	13.27	13.32
MgO	7.18	6.34	6.96	5.14	7.71	11.85
CaO	7.34	4.31	8.72	3.22	17.7	7.22
Na ₂ O	4.09	4.89	4.27	5.18	1.22	1.41
K ₂ O	1.08	0.56	1.51	0.98	1.36	0.28
P ₂ O ₅	0.27	0.24	0.1	0.28	0.1	0.06
Total C	tr	0.67	1.56	0.23	5.89	2.88
Total	100.01	100.08	99.72	99.86	99.86	98.87
Y	22	19.8	29.1	26.8	15.7	11.4
Zr	139	128.3	138.4	155.5	67.1	50.2
Nb	12.9	15.6	16.1	18.3	7.5	3.6

tr = trace

Philips PW1400 spectrometer; major elements (Rh Ka), trace elements (W Ka), counting times between 10 and 100 seconds. Total carbon analyses; Strohlein Coulomat 702.



- Carbonate solubility curves constructed for T=300°C, P=1kb and I=1.0, T=300°C, I=0.25 and T=250°C, I=1.0
- The magnetite stability field has been replaced by chlorite (Barton et al. 1977)
- Total S=0.01 m, aCO₂+CH₄=750b, log mCa⁺²=-3, log mK⁺=-1.3 (Walsh et al. 1988)
- Log Sb molality values (Akeret 1953)

Figure 4: pH-f₀2 mineral stability diagram.

Both mechanisms may effect a change to higher fluid pH and f₀2, creating a chemical environment in which the uptake and transport

of Sb in the metasomatic fluid is possible (Figure 4) (Akeret, 1953, Wood, 1989). The occurrence of apatite in veinlets within the carbonatised rock suggests that F⁻ and PO₄³⁻ were also important in the fluid.

GEOCHEMISTRY OF CARBONATISED METABASITES

A reconnaissance study employing samples selected with reference to shears, intra-basite micro-breccias and zones of intense carbonatisation (Figure 1) were subdivided upon the basis of petrographic and field characteristics. Groups I - V represent progressive stages in the structural/metamorphic development of one metabasite, from "unaltered" (Group I) to microbreccia (Group V), whilst Group VI contains samples from other metabasites at Port Quin (Table 2).

The geochemical responses to carbonatisation and deformation suggest;

- the availability of reactive fluids to mobilise elements commonly considered most refractory,
- volume/mass changes in the metabasite during metasomatism.

Of interest is the behaviour of HFS elements (Zr, Nb, Y, Ti) (generally incompatible and the least mobile) and Al, under conditions of progressive carbonatisation and deformation. Changes in these element abundances and ratios cannot always be easily attributed to simple addition or removal as this suggests extreme rates of transfer, deemed unlikely from their relatively immobile nature. Instead it may be more correct to consider changes in rock volume/mass during carbonatisation to account for these differences.

The bivariate plots illustrate these changes and indicate the relative mobility between the different elements. Perfectly immobile elements plot along a common line that passes through both the bulk composition and the origin, and retain constant inter-element ratios whether they are unaltered or altered. Construction of alteration lines assist to characterise the style of compositional change within the rock. Providing the original abundances of the incompatible elements can be reliably estimated, the position along an alteration line defined by the adjusted abundances will be determined by the degree of element mobility or whether material has been gained or lost during alteration. If relative immobility of the above elements is proved, the addition of further material to the rock (i.e. volume gain) will effect dilution and samples will plot closer to the origin (e.g. Finlow-Bates and Stumpfl, 1981). Conversely, if material is subtracted during alteration (i.e. volume loss), element concentration occurs and samples will plot further from the origin.

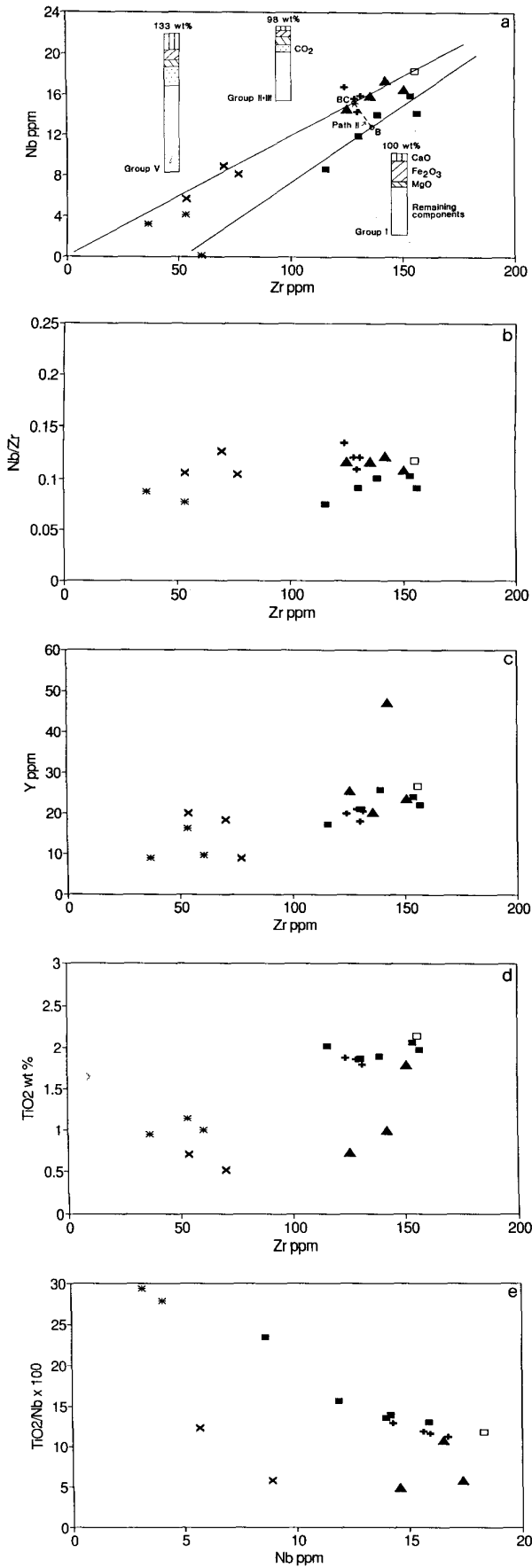


Figure 5: Zr-Nb, Zr-Nb/Zr, Zr-Y, Zr-TiO₂ and Nb-TiO₂/Nb x 100 plots.

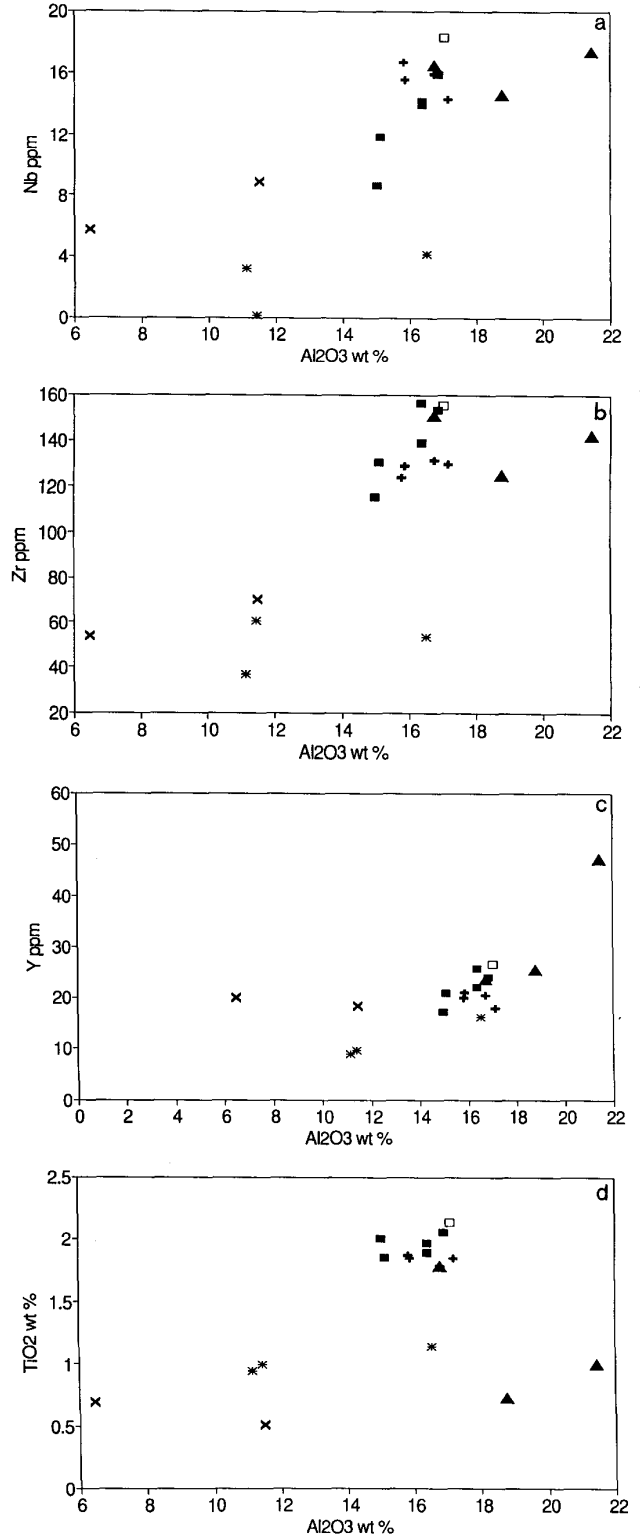
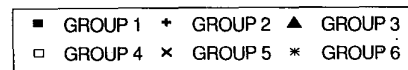


Figure 6 Al₂O₃-Nb, Al₂O₃-Zr, Al₂O₃-Y and Al₂O₃-TiO₂ plots.



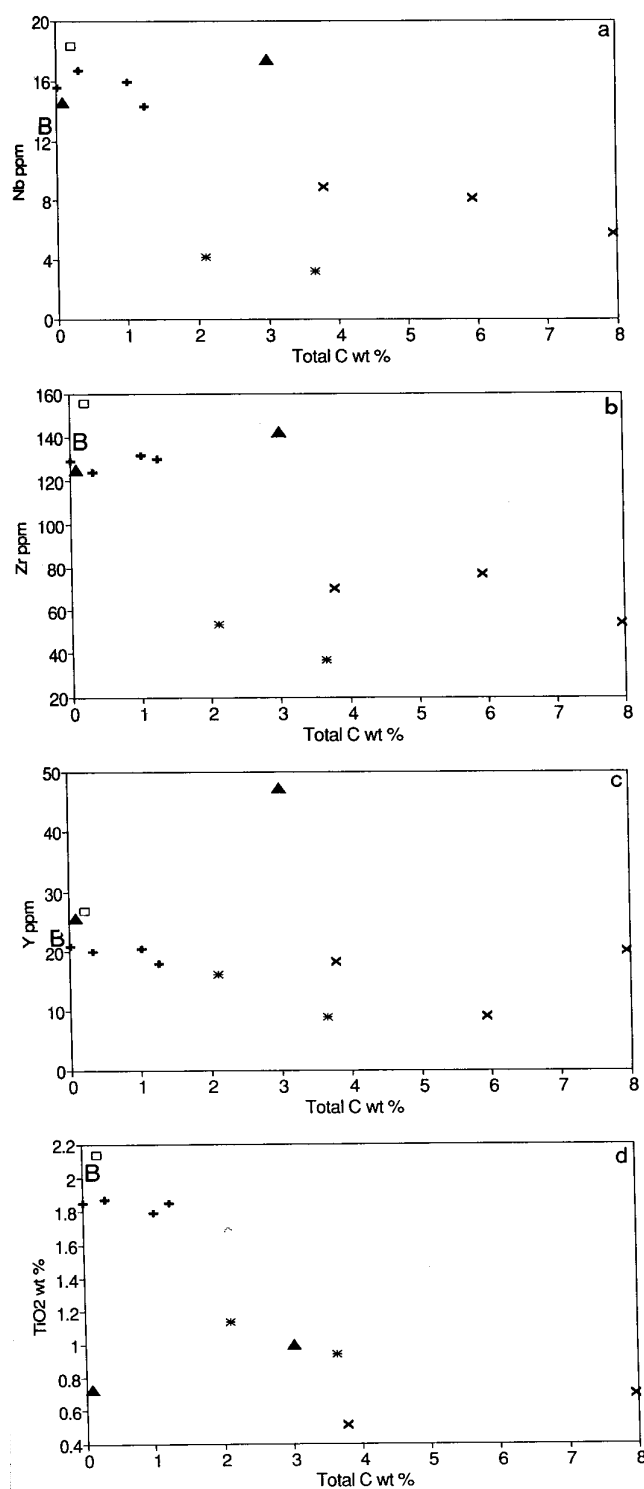


Figure 7: Total C-Nb, Total C-Y and Total C-TiO₂ plots

If mobility is proved, the possible mechanisms of uptake and transportation of the more mobile elements constrain the chemistry and redox state of the metasomatic fluid and provide evidence regarding the conditions of Sb transport.

RESULTS

Zr-Nb relationships

A comparison between the averaged values for Nb and Zr shows Nb to be more effectively concentrated during carbonatisation and

deformation, and perhaps shows greater tendency toward immobility. Figure 5a reveals two trends distinguishing carbonatised metabasites from "unaltered" metabasites via a fall in Zr/Nb ratio. Figure 5b confirms an enrichment in Nb without a corresponding increase in Zr, showing also the constancy in Nb/Zr ratio in the carbonatised samples. Two geochemical pathways are possible;

- addition of Nb at constant mass (i.e. Zr abundance is maintained),
- concentration of Nb with loss of mass (where mass loss is accomplished via a process effective in mobilising Zr).

Hynes (1980), Ludden et al. (1984) and Moritz and Crockett (1991) cite evidence linking the mobility of Zr with alkaline fluids (i.e. those which have lost much of their CO₂) whilst Giere (1989) indicates PO₄³⁻ as an additional influence upon Zr mobility. In combination with volume calculations (Figure 5a), this suggests that removal of Zr is more likely than addition of Nb during incipient carbonatisation. The reconstruction of pathway ii. is shown in Figure 5a.

Carbonatisation effectively displaces the bulk Zr/Nb ratio for "unaltered" metabasites (B), to a point (BC) upon a "carbonatisation line" (Zr/Nb = 8.5). The closest estimate for this point is the cluster defined by weakly carbonatised metabasites (Group II). The Zr/Nb ratio for samples along the "carbonatisation line" is approximately constant indicating little relative mobility between Nb and Zr once carbonatisation had commenced. A shift upslope from point BC to groups III and IV describes a concentration of Nb and Zr at constant Zr/Nb; this might best be achieved under a further loss in mass. Group V, representing samples with advanced carbonatisation, show strong depletion in Nb and Zr at constant Zr/Nb and reflect dilution under conditions of mass gain in micro-breccias.

Zr-Y relationships

Correlation between groups I, II, III and IV (Figure 5c) indicates that Zr and Y generally behaved similarly with respect to each other; consequently Nb/Y is also higher in the carbonatised samples. The positive effect of alkalinity upon Zr mobility (Murphy and Hynes 1986, Giere 1989) is also applicable to Y, whereby transport is made permissible via complexing of Y³⁺ with CO₃²⁻ (Hynes, 1980). However, a similar geochemical pathway for Zr and Y cannot be supported from Group V, and an anomalous sample in Group III, which both contain higher Y/Zr indicating a disparity in the more carbonatised samples (Total C = 3–8 wt %).

In Group V, the lowered Zr abundance and higher Y/Zr are consistent with dilution via a gain in mass, as described in Figure 5a, by a mechanism known to permit an increase in Y relative to Zr. The ability for Y to complex with CO₃²⁻ may account for this, and likewise, the Y enrichment in the most carbonated sample in Group III. It appears that Y/Zr is influenced by the fluid chemistry which regulated the rate of element transport.

The behaviour of TiO₂

Close similarity between TiO₂ and Zr abundances and constant Zr/TiO₂ in group I and II (Figure 5d) may suggest the Ti-bearing minerals (e.g. augite, sphene, ilmenite) also acted as principal Zr carriers in these rocks. Zr/TiO₂ increases with advanced carbonatisation (groups III and V) suggesting that these elements behaved differently during carbonatisation and deformation, a trend also shown by Hynes (1980), and MacLean and Kranidiotis (1987) in carbonatised metabasites of greenschist facies. Extensive degradation of the Ti-bearing minerals and their replacement by Cl carbonate suggests that this disparity was best effected by agents responsible for this widespread alteration.

Figure 5e indicates progressive depletion in TiO₂/Nb through groups I, II and III. This is attributed to the removal of Ti under conditions of mass loss permitting the concentration of Nb which acted as a relatively immobile element. The resemblance between Figure 5e and the Nb-Zr/Nb plot (not illustrated) lends support for

the retention of Zr in Ti-bearing minerals. Ti, Zr and Y all appear to show some degree of mobility with carbonatisation and deformation. Evidently these elements, comparatively immobile under conditions of seafloor alteration and very low grade metamorphism (Floyd, 1982; Robinson and Sexton, 1987) behaved very differently under conditions of progressive carbonatisation.

The lower abundances of Nb, Zr, Y and Ti shown by metabasites in Group VI is considered to reflect variable primary element abundances in the different metabasites at Port Quin, suggesting that original magmatic abundances control to some degree the levels remaining post-carbonatisation.

The variation in Al₂O₃

Al is generally concentrated in the residual phases within altered rocks and shows tendency to be conserved in metasomatic haloes (Bohlke, 1989) and zones of hydrothermal alteration (MacLean and Kranidiotis, 1987). Except under very low pH, Al is less soluble and thereby less mobile than other elements, hence its wide use in mass balances (e.g. Grant, 1986; Gresens, 1967).

A sympathetic relationship is described between Al₂O₃ and Nb, Zr and Y in Group I, whereas a flatter slope is described between Al₂O₃-TiO₂ (Figures 6a to 6d). A general case is apparent involving an increase in Al₂O₃/"incompatible" ratio through groups I → II → III with carbonatisation and deformation, prior to a depletion of Al in Group V. Such behaviour is similar to that identified for Nb, except that progressively higher averaged Al₂O₃/Nb implies Al is less mobile. Total immobility cannot be assumed as successive stages of chlorite formation imply short range movement although removal from the system is not detected on the scale of samples used.

Element behaviour against total C

The C analysed was determined to be almost wholly inorganic C and generally increased in abundance with the degree of deformation observed petrographically. Figures 7a to d show that carbonatisation is best developed in brittle deformed metabasites (Group V), where it is accompanied by sulphide/sulphosalt mineralisation. The y-axis symbol "B" represents the averaged bulk abundance for each particular element in Group I, from which the initial concentration of Nb and Al (Group II, total C-Al₂O₃ plot not illustrated) reflects mass loss incurred during incipient carbonatisation. The depletion of Zr, Ti and Y at this stage implies their limited mobility as described above. The sharp fall in Nb, Zr and Al₂O₃ (Group V), attributed to dilution via mass gain in the formation of microbreccias, is not shown by Y or TiO₂. Y shows a smoother decrease, possibly reflecting its greater mobility, whilst the abrupt decrease in Ti from "B" to Group II, and again in Group III, may reflect loss of Ti at a stage prior to extensive carbonatisation.

The relationship between carbonatisation and the degree of deformation is clearly inconsistent, such that some areas in the metabasite appear to have remained permanently closed to carbonatisation. This relationship is exemplified by a ductile deformed metabasite sample (Group IV), located adjacent to a quartz vein without carbonate, which shows a low total C abundance. This might suggest that the rock fabric was acquired prior to, and was not affected during, carbonatisation; that low permeabilities in the basalt precursor were retained during deformation and carbonatisation, or that carbonate bearing fluid was not admitted to the fracture/vein. In any event the geochemistry of this group generally follows that of the carbonatised samples and demonstrates the need to study metasomatic effects preceding carbonatisation and the role played by ductile deformation in producing chemical changes.

Molar CO₂/CaO

Molar CO₂/CaO ratios serve as a useful index of alteration in carbonatised rocks and indicate the dolomite/calcite ratio (Davies *et*

al, 1990; Moritz and Crocket, 1991). In uncarbonated rocks mCO₂/CaO = 0 while carbonatised metabasites with mCO₂/CaO = 1 characterise those in which all CaO occurs in the form of calcite. Values between 0 and 1 express the proportion of total CaO that exists as calcite and when >1 imply additional carbonate minerals (e.g. dolomite). mCO₂/CaO values for metabasites at Port Quin lie between 0.01 and 1.80 which give a dol/dol+cal ratio between 0.13 - 1.02. Values >1 agree well with the distribution of cold acid insoluble carbonate (ferroan dolomite) in the metasomatic rock.

DISCUSSION AND CONCLUSIONS

The widespread development of carbonatised metabasites in north Cornwall suggest these were both receptive to and reacted with a CO₂-rich metasomatic fluid. They afforded favourable sinks for discharges of fluid which entered via brittle-ductile structures, and experienced volume changes to accommodate mineral transformations during metasomatism and deformation. Broad constraints upon redox conditions in the metasomatic fluid and the mechanism of carbonate precipitation are indicated from the mineralised and brecciated metabasite at Port Quin.

The sulphide-sulphosalt paragenesis in the metabasite appears in broad agreement with that observed in vein deposits at Port Quin and elsewhere in north Cornwall. Initial conditions are described by an area close to the Mu-K fsp boundary in the pyrite stability field. Relict, oxidised pyrites indicate higher fO₂ conditions outside this field during the early stages of carbonatisation. Pervasive replacement by carbonate implies that this excursion also described a move to higher pH and intersected the carbonate solubility curve. Successive chlorite-carbonate cycles require repeated variation in fluid conditions, as might be described by areal changes in the carbonate stability field in response to changes in temperature or ionic strength of the fluid (Walsh *et al.*, 1988). The variation in ionic concentration required to effect these changes may be brought about by fluctuations in CO₂ concentration.

Fluid inclusion evidence suggests that the concentration of CO₂ was influenced by immiscibility in the metasomatic fluid and effected a strong control over carbonate precipitation (Clayton, 1992). The preferred mechanism involves separation in the fluid, triggered by hydraulic cracking of the metabasite in response, to high fluid pressures. As these breccias are intensely carbonatised, the high pressures were probably augmented by high PCO₂ and released prior to carbonate precipitation, resulting in adiabatic decompression of the fluid, CO₂ outgassing and pervasive carbonatisation outward from the breccia.

CO₂ outgassing and H⁺ extraction through chlorite precipitation generated mild fluid alkalinity which is detected in the mobility of some high field strength elements (Zr, Y, Ti). Hynes (1980), Ludden *et al.* (1984) and Murphy and Hynes (1986) examined the mobility of Zr, Y and Ti in rocks altered by fluids with high CO₂ activities and indicated that CO₃²⁻ acted as an important ligand. In studies of present day heated groundwaters, Henderson *et al.* (1987) have described hot, alkaline spring waters enriched in bicarbonate and fluoride containing high concentrations of Zr. Additionally, Gere (1989) indicated the mobility of Ti and Zr to be favoured by relatively high activities of F⁻ and PO₄³⁻, whilst Alderton *et al.* (1980) noted W to have some influence. This behaviour provides a direct contrast with the general immobility of Zr, Y and Ti in aqueous solutions.

Alkaline solutions are also known to transport hydroxide and thio-complexes of Sb (Akeret, 1953; Kolpakova, 1982). Solubility studies indicate thio-antimony species to be important for the transport of Sb in near-neutral to alkaline, sulphide-rich solutions with SbS₂⁻, SbS₃³⁻, Sb₂S₄⁴⁻ and/or their protonated equivalents the most likely species in hydrothermal solutions (Spycher and Reed, 1989; Wood, 1989). The most probable stoichiometries of the protonated thio-antimony complexes are H₂Sb₂S₄ and HSb₂S₄⁻, of which only HSb₂S₄⁻ is stable within the pH range of typical geochemical systems (Spycher and Reed, 1989).

In addition, Wei and Saukov (1961) successfully precipitated Sb_2S_3 from alkaline sulphide solutions, citing that the important factor causing precipitation was neutralisation, caused mainly by the action of CO_2 and oxidation.

Basalt carbonatisation and the generation of mild alkalinity in the metasomatic fluid offers a possible mechanism for Sb-sulphosalt mineralisation in the metabasite at Port Quin. The close comparison of fluid compositions and mineralogical characteristics between the metasomatic deposit and Sb vein mineralisation at Port Quin may demonstrate a link between basalt carbonatisation and Sb-sulphosalt mineralisation in north Cornwall.

Acknowledgements. A research studentship (Exeter Univ.) and support from the British Geological Survey is gratefully acknowledged. Carbon analyses were undertaken at Oxford Univ. by M.K. Durkin.

REFERENCES

- AKERET, R. 1953. Ueber die Löslichkeit von Antimon (3) Sulfid. Unpublished PhD thesis, Prom. Nr. 2271, Eidgenössische Technische Hochschule, Zurich.
- ALDERTON, D.H.M., PEARCE, J.A. and PORRIS, P.J. 1980. Rare earth mobility during granite alteration: Evidence from south-west England. *Earth and Planetary Science Letters*, **49**, 149-165.
- AYDAL, D. 1990. Gold bearing listvenites in the Arac Massif, Kastamanu, Turkey. *Terra Nova*, **2**, 43-52.
- BARTON, P.B.Jr., BETHKE, P.M. and ROEDDER, E. 1977. Environment of ore deposition in the Creede mining district, San Juan Mountains, Colorado: Part III. Progress toward interpretation of the chemistry of the ore-forming fluid for the OH vein. *Economic Geology*, **72**, 1-24.
- BOHLKE, J.K. 1989. Comparison of metasomatic reactions between a common CO_2 -rich vein fluid and diverse wall-rocks: Intensive variables, mass transfers and Au mineralization at Alleghany, California. *Economic Geology*, **84**, 291-327.
- BUISSON, G. and LEBLANC, M. 1986. Gold-bearing listvenites (carbonatised ultramafic rocks) from ophiolitic complexes. In: Metallogeny of basic and ultrabasic rocks. Eds: M. J. Gallagher, R. A. IXER, C. R. NEARY and H. M. PRITCHARD, *Institution of Mining and Metallurgy*, 121-131.
- CLAYTON, R.E. 1992. Antimony mineralisation and other sulphide deposits in the northern zone of the Trevone Basin, north Cornwall. *Unpublished Ph.D. thesis*, University of Exeter.
- CLAYTON, R.E., SCRIVENER, R.C. and STANLEY, C.J. 1990. Mineralogical and preliminary fluid inclusion studies of lead-antimony mineralisation in north Cornwall. *Proceedings of the Ussher Society*, **7**, 258-262.
- DAVIES, J.F., WHITEHEAD, R.E., HUANG, J. and NAWARATNE, S. 1990. A comparison of progressive hydrothermal carbonate alteration in Archaean metabasalts and metaperidotites. *Mineralium Deposita*, **25**, 65-72.
- FINLOW-BATES, T. and STUMPFL, E.F. 1981. The behaviour of the so-called immobile elements in hydrothermally altered rocks associated with volcanogenic submarine-exhalative ore deposits. *Mineralium Deposita*, **16**, 319-328.
- FLOYD, P. 1982. Chemical variation in Hercynian basalts relative to plate tectonics. *Journal of the Geological Society of London*, **139**, 505-520.
- GIERE, R. 1989. Hydrothermal mobility of Ti, Zr and REE: Examples from the Bergell and Adamello contact aureoles (Italy). *Terra Nova*, **2**, 60-67.
- GRANT, J.A. 1986. The isocon diagram - A simple solution to Gresens' equation for metasomatic alteration. *Economic Geology*, **81**, 1979-1982.
- GRESENS, R.L. 1967. Composition-volume relationships of metasomatism. *Chemical Geology*, **2**, 47-65.
- HENDERSON P, PICKFORD, M. and WILLIAMS, C.T. 1987. A geochemical study of rocks and spring waters at Kanam and Kanjera, Kenya, and the implications concerning element mobility and uptake. *Journal of African Earth Sciences*, **6**, 221-227.
- HYNES, A. 1980. Carbonatization and mobility of Ti, Y and Zr in Ascut Formation Metabasalts, S.E. Quebec. *Contributions to Mineralogy and Petrology*, **75**, 79-87.
- KOLPAKOVA, N.N. 1982. Laboratory and field studies of ionic equilibria in the Sb_2S_3 - H_2O - H_2S system. *Geochemistry International*, **19**, 46-54.
- LUDDEN, J.N., DAIGNEAULT, R. ROBERT, F. and TAYLOR, R.P. 1984. Trace element mobility in alteration zones associated with Archean Au lode deposits. *Economic Geology*, **79**, 1131-1141.
- MACLEAN, W.H. and KRANIDIOTIS, P. 1987. Immobile elements as monitors of mass transfer in hydrothermal alteration: Phelps Dodge massive sulphide deposit, Matagami, Quebec. *Economic Geology*, **82**, 951-962.
- MORITZ, R.P. and CROCKET, J.H. 1991. Hydrothermal wall-rock alteration and formation of the gold-bearing quartz-fuchsite vein at the Dome Mine, Timmins area, Ontario, Canada. *Economic Geology*, **86**, 620-643.
- MURPHY, J.B. and HYNES, A.J. 1986. Contrasting secondary mobility of Ti, P, Zr, Nb and Y in two metabasaltic suites in the Appalachians. *Canadian Journal of Earth Sciences*, **23**, 1138-1144.
- PLOSHKO, V.V. 1963. Listvenitization and carbonatization at terminal stages of Urushten igneous complex, North Caucasus. *International Geology Review*, **7**, 446-463.
- RICE-BURCHALL, B. 1991. Petrology and geochemistry of basic volcanics, north Cornwall. *Unpublished Ph.D. thesis*, University of Keele.
- ROBINSON, D. and SEXTON, D. 1987. Geochemistry of the Tintagel Volcanic Formation. *Proceedings of the Ussher Society*, **6**, 523-528.
- SPYCHER, N.F. and REED, M.H. 1989. As(III) and Sb(III) sulphide complexes: an evaluation of stoichiometry and stability from existing experimental data. *Geochimica et Cosmochimica Acta*, **53**, 2185-2194.
- WALSH, J.F., KESLER, S.E., DUFF, D. and CLOKE, P.L. 1988. Fluid inclusion geochemistry of high grade, vein-hosted gold ore at the Pamour Mine, Porcupine Camp, Ontario. *Economic Geology*, **83**, 1347-1367.
- WEI, D. and SAUKOV, A.A. 1961. Physicochemical factors in the genesis of antimony deposits. *Geokhimiya*, **6**, 510-516.
- WOOD, S.A. 1989. Raman spectroscopic determination of the speciation of ore metals in hydrothermal solutions: I. Speciation of antimony in alkaline sulphide solutions at 25°C. *Geochimica et Cosmochimica Acta*, **53**, 237-244.